



May 27, 2022

The LHCb prompt charm triggers

PATRICK SPRADLIN

ON BEHALF OF THE LHCb COLLABORATION

*School of Physics and Astronomy
University of Glasgow, Glasgow, UK*

The LHCb experiment has fully reconstructed close to 10^9 charm hadron decays—by far the world’s largest sample. During the 2011-2012 running periods, the effective pp beam crossing rate was 11-15 MHz while the rate at which events were written to permanent storage was 3-5 kHz. Prompt charm candidates (produced at the primary interaction vertex) were selected using a combination of exclusive and inclusive high level (software) triggers in conjunction with low level hardware triggers. The efficiencies, background rates, and possible biases of the triggers as they were implemented will be discussed, along with plans for the running at 13 TeV in 2015 and subsequently in the upgrade era.

PRESENTED AT

The 6th International Workshop on Charm Physics
(CHARM 2013)
Manchester, UK, 31 August – 4 September, 2013

1 Introduction

The LHCb experiment has rapidly become one of the foremost high-precision flavor physics experiments, collecting the world’s largest samples of several decay modes of c and b -hadrons (*e.g.*[1, 2]). This success would have been impossible without LHCb’s flexible and efficient trigger system.

The task of rapidly selecting which events will be stored permanently for subsequent analysis and which will be discarded forever—triggering—presents a formidable challenge in the high-energy hadronic collision environment of the Large Hadron Collider (LHC). In 2012 the LHCb detector witnessed pp collisions with a center-of-mass energy of $\sqrt{s} = 8$ TeV at a mean instantaneous luminosity of approximately $4 \times 10^{32} \text{ cm}^{-2}\text{s}^{-1}$. Given that the heavy flavor hadron production cross-sections into the LHCb acceptance were measured to be $\sigma_{b\bar{b},\text{acc}} = 75.3 \pm 14.1 \mu\text{b}$ [3] and $\sigma_{c\bar{c},\text{acc}} = 1419 \pm 134 \mu\text{b}$ [4] for pp collisions at $\sqrt{s} = 7$ TeV, the rate of heavy flavor production into the LHCb acceptance exceeded 30 kHz for b -hadrons and 600 kHz for c -hadrons. Because events are written to permanent storage at just 3-5 kHz, the trigger must be highly selective even among events with a real heavy-flavor hadron.

This article discusses the structure and performance of the trigger components for selecting events that contain open charm hadrons—the first and fundamental building block for most precision charm measurements at LHCb. We also sketch prospective improvements to the trigger that will extend our physics reach when the LHC returns to operation after its first long shutdown period (LS1) and in the era of the upgraded LHCb detector.

2 Detector

The LHCb detector [5] is a single-arm forward spectrometer covering the pseudorapidity range $2 < \eta < 5$, designed for the study of particles containing b or c quarks. Charm hadron triggering uses information from each of the detector subsystems. The detector includes a high-precision tracking system consisting of a silicon-strip vertex detector surrounding the pp interaction region, a large-area silicon-strip detector located upstream of a dipole magnet with a bending power of about 4 Tm, and three stations of silicon-strip detectors and straw drift tubes placed downstream. The combined tracking system provides a momentum measurement with relative uncertainty that varies from 0.4% at 5 GeV/ c to 0.6% at 100 GeV/ c , and impact parameter resolution of 20 μm for tracks with large transverse momentum. Different types of charged hadrons are distinguished by information from two ring-imaging Cherenkov detectors [6]. Photon, electron, and hadron candidates are identified by a calorime-

ter system consisting of scintillating-pad and preshower detectors, an electromagnetic calorimeter and a hadronic calorimeter. Muons are identified by a system composed of alternating layers of iron and multiwire proportional chambers [7].

3 Trigger overview

Although the global structure of the LHCb trigger system—a hardware trigger system followed by a full detector readout and one or more layers of software triggers—has remained unchanged since its initial design [8], the implementation continues to evolve. The trigger system as it performed in 2011 is described in detail in Ref. [9], but the interval between 2011 and 2012 saw the introduction of a major new feature, HLT deferral (Sec. 4). The steady evolution of the trigger has led to and has been encouraged by an expansion of LHCb’s physics program. Relative to the initial design, the 2012 LHCb trigger processed twice the instantaneous luminosity of events ($4 \times 10^{32} \text{ cm}^{-2}\text{s}^{-1}$ vs. $2 \times 10^{32} \text{ cm}^{-2}\text{s}^{-1}$) with a much greater complexity (a mean of 1.6 visible pp interactions per visible bunch crossing vs. 0.4) and recorded events to permanent storage at over twice the rate (5 kHz vs. 2 kHz). As a consequence, LHCb is making an impact in areas far outside its initial core physics program [10, 11], particularly in the realm of charm physics. Though charm physics measurements were previously absent from LHCb’s primary goals, approximately 40% of the trigger output is now dedicated to them.

Figure 1 outlines the structure of the trigger system for 2012 data collection. The chain begins with a bunch crossing in which a bunch of protons from each of the counter-rotating beams of the LHC meet at the LHCb interaction point. The separation between successive potential sites for bunches of protons in the beams of the LHC is 25 ns, thus bunch crossings may occur at a maximum rate of 40 MHz [12]. In much of 2012 the actual bunch crossing rate at the LHCb interaction point was 11-15 MHz.

The first layer of triggering happens in bespoke hardware. Since the maximum rate at which the full detector response can be digitized and read out is 1 MHz, the purpose of this level-0 trigger system (L0) is to select just 1 MHz of potentially interesting

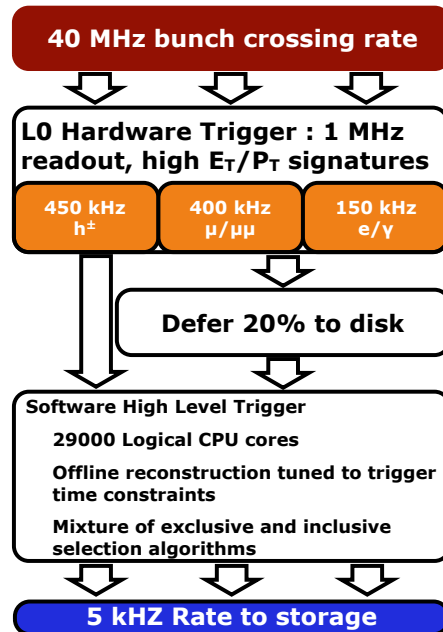


Figure 1: A diagrammatic overview of the trigger structure.

events from the 11-15 MHz of bunch crossings. L0 analyzes the response of selected subdetectors to evaluate measures of event complexity and to identify signatures of particles with large momentum components transverse to the pp collision axis (p_T). It contains a number of independent parallel configurable channels that are tuned to balance the requirements of the physics program and the readout constraint. If any one of the channels returns a positive decision, the full detector response is digitized, read out, and recorded to the temporary storage of the Event Filter Farm (EFF), a large farm of multiprocessor computers, until the trigger processing is complete and a final decision made on the fate of the event.

Most of the events accepted by L0 and transferred to the EFF are processed immediately by the subsequent and final triggering layer, the High Level Trigger (HLT). For 20% of the events the HLT processing is deferred until the interfill period (see Sec. 4). HLT is implemented in software that runs on the EFF. Due to limitations of computing resources available for permanent storage and data analysis, the rate at which events are accepted for permanent storage is restricted to 5 kHz.

Internally, HLT is segmented into two sequential stages of processing, HLT1 and HLT2. Each stage is composed of several independent parallel channels (lines) that are sequences of event reconstruction algorithms and selection criteria. Each line executes its sequence of elements either until the decision of the line is known to be negative, *e.g.*, by the failure of a reconstruction element or selection criterion, or until the sequence is complete and the event accepted by the line. The lines of HLT2 are executed only for events that are accepted by at least one of the lines of HLT1. Events accepted by at least one HLT2 line are preserved in permanent storage.

The lines of HLT1 are simple selections based on the properties of one or two reconstructed tracks. The lines of HLT2 can be quite sophisticated, incorporating complicated reconstruction elements and multivariate discriminants, and are generally tailored to the requirements of a group of physics analyses. The lines of HLT2 are generally better suited to the needs of LHCb measurements than those of HLT1. However, they also require substantial computing resources. The EFF has the computing power to execute the lines of HLT2 on only a fraction of the L0-accepted events. Thus the two-stage structure of HLT is a compromise, with HLT1 rapidly selecting a subset of the L0-accepted events to be further analyzed by HLT2.

4 HLT deferral

The trigger system in 2012 featured a new facility for deferring HLT processing for a fraction of the events accepted by L0. This represents a significant improvement in the efficiency with which the EFF is used. Prior to the implementation of HLT deferral, all events were processed immediately after they were transferred to the EFF. In normal operation, the beams of the LHC are dumped when their intensity

decays below some threshold. New beams with renewed intensity are then injected and accelerated to the target energy before collisions resume. This interfill period in which no recordable collisions occur can take a few hours during which the EFF would remain largely idle. With the HLT deferral system, most events are processed immediately, as before, but a configurable fraction of the incoming events are cached in EFF storage instead of processed. During the interfill period, HLT processes these cached events. The net result is a more efficient use of the EFF that effectively increased the available computing power by approximately 20% in 2012.

5 Performance measures

We measure the performance of trigger lines in data with the method described in Ref. [9]. The data sets for the measurements are collections of ‘offline’ candidate decays that have been reconstructed by LHCb’s analysis software from the collected events. We require that at least one channel at each level of the trigger accepted each event independently of the offline candidate in order to mitigate biases due to the *de facto* triggering of the events.

In order to measure the efficiency with which these offline candidate decays satisfy the criteria of a trigger line under investigation, we must compare the underlying information from the detector that was used in reconstructing the offline candidate to that used in the decision of the trigger line. This is done by a direct comparison of the set of detector elements—the strips, straws, cells, and pads of the sub-detectors—that contributed to each. As most HLT1 and HLT2 lines are based on sets of reconstructed tracks, this is effectively a comparison of the set of tracks constituting the offline candidate decay and the set of tracks used by the line. We classify an offline candidate as Triggered On Signal (TOS) for a given trigger line if the set of detector elements that was used in its reconstruction is sufficient to satisfy the selection criteria of that line. An offline candidate is classified as Triggered Independently of Signal (TIS) for a given trigger line if the set of detector elements that was used in its reconstruction is disjoint with at least one of the combinations of elements that led to a positive decision by that trigger line, that is, if the rest of the event excluding the offline signal candidate was sufficient to satisfy the criteria of that line. These are not mutually exclusive classifications. A given offline candidate decay can be both TOS and TIS with respect to a given trigger line as there may be multiple sets of detector elements whose response led to a positive decision for the line.

The offline candidate decays of the data sets for trigger performance are TIS with respect to at least one physics line at each level of the trigger. The candidates of these data sets are largely unbiased by the trigger line under investigation. A subset of these candidates will also be TOS with respect to the target line. After determining

Table 1: Mean ϵ^{TOS} efficiencies of L0Hadron for selected charm hadron decays.

Decay mode	Mean ϵ^{TOS}
$D^0 \rightarrow K^- \pi^+$	0.26894 ± 0.00069
$D^+ \rightarrow K^- \pi^+ \pi^+$	0.15766 ± 0.00016
$D^{*+} \rightarrow \pi^+ D^0 (K^- \pi^+ \pi^+ \pi^-)$	0.22045 ± 0.00043

the number of signal decays in the set of TIS candidates (N^{TIS}) and of its TOS subset ($N^{\text{TOS} \wedge \text{TIS}}$), we define our measure of the performance of a line as its TOS efficiency, $\epsilon^{\text{TOS}} = N^{\text{TOS} \wedge \text{TIS}} / N^{\text{TIS}}$.

The TOS efficiency defined in this way should be considered a relative measure of performance rather than an absolute efficiency. It is sensitive to the criteria with which the set of offline candidate decays were selected. Further, the TIS classification includes some bias due to the pairwise production mechanisms of heavy hadrons. Despite these limitations, ϵ^{TOS} is an excellent measure of the relative performance of a trigger line.

In Sections 6 to 8 we will show ϵ^{TOS} for offline reconstructed decays of three charmed hadrons to final states involving kaons and pions: $D^0 \rightarrow K^- \pi^+$, $D^+ \rightarrow K^- \pi^+ \pi^+$, and $D^{*+} \rightarrow \pi^+ D^0 (K^- \pi^+ \pi^+ \pi^-)$. The corresponding charge-conjugate decays are implied here and throughout the remainder of this article. These modes were selected due to their large abundance and in order to show the dependence of trigger efficiencies on the multiplicity of the final state. Rare open charm hadron decays to final states with two muons are expected to have a significantly better performance, comparable to that of J/ψ decays (see Ref. [9]). However, their ϵ^{TOS} performance cannot be evaluated until sufficiently large samples are available. All of the plots and performance estimates in the following sections are based on data collected by LHCb in 2012 in pp collisions at $\sqrt{s} = 8$ TeV.

6 L0 performance

The L0 hardware trigger system is described more completely in Refs. [5, 9]. The decisions of the parallel channels are based on comparisons of a small number of estimated quantities to specified configurable thresholds. The primary physics quantities are the estimated transverse momenta for track segments in the muon system and estimated transverse energy (E_{T})* for clusters in the calorimeter system. The overall activity in the scintillating-pad detector enters many L0 channels as a proxy measure of event complexity.

*For a calorimeter cell centered at polar coordinates $\vec{x} = (r, \theta, \phi)$ in the LHCb coordinate system in which the origin is at the center of the pp interaction envelope and the z -axis is the laboratory-frame collision axis, a measured deposited energy of E corresponds to $E_{\text{T}} = E \sin \theta$.

The primary channel of interest for hadronic decays of charmed hadrons is the single-cluster hadron line `L0Hadron`. It accepts events that have a scintillating-pad detector activity below a certain threshold and that contain at least one cluster in the hadron calorimeter that has a total transverse energy in all calorimeters of $E_T > 3.5$ GeV. In 2012, approximately 45% of the events accepted by L0 were accepted by `L0Hadron`. Figure 2 shows ϵ^{TOS} of `L0Hadron` as a function of signal hadron p_T for $D^0 \rightarrow K^- \pi^+$, $D^+ \rightarrow K^- \pi^+ \pi^+$, and $D^{*+} \rightarrow \pi^+ D^0 (K^- \pi^+ \pi^+ \pi^-)$ decays. It also shows ϵ^{TOS} of `L0Hadron` for two hadronic B decay modes, $B^+ \rightarrow \pi^+ D^0 (K^- \pi^+)$ and $B^0 \rightarrow K^+ \pi^-$. The efficiencies of `L0Hadron` are strongly dependent on the p_T of the signal hadron. Charm hadrons are predominantly produced in the region of low efficiency [4], thus the mean efficiency for the set of offline candidate decays is correspondingly low, as shown in Table 1. One of the important ways in which the redesigned trigger for the upgraded LHCb detector will benefit LHCb’s charm physics program by removing the limitations of the L0 system (see Section 9.2).

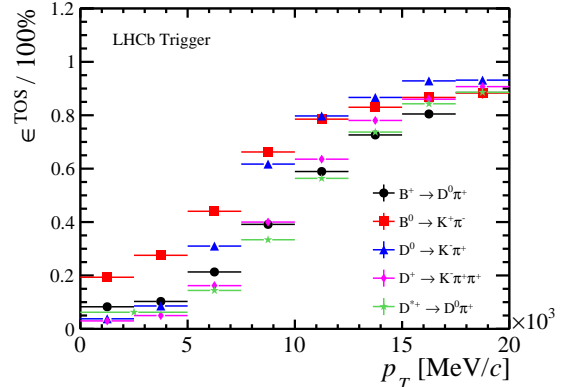


Figure 2: The efficiencies of `L0Hadron` for various reconstructed decay modes as functions of p_T of the signal B and D candidate based on $\sqrt{s} = 8$ TeV data collected in 2012.

7 HLT1 performance

HLT1, the initial stage of the HLT software trigger, is composed of parallel independent lines—sequences of processing steps that include reconstruction elements and selection criteria. The decisions of the L0 channels are available to HLT1 lines, so the trigger history of an event can enter the decision-making process of a line.

Although the lines of HLT1 are independent, most lines begin with a fast reconstruction of pp primary interaction vertexes (PVs) and charged particle tracks that is common to all lines that use it. The details of this fast reconstruction are fully described in Ref. [9]. Most HLT1 lines are simple selections based on the properties of one or two of these reconstructed tracks. The single displaced-track line `Hlt1TrackAllL0`, which is the primary HLT1 line of interest for charmed hadron decays to hadronic final states, is of this type. `Hlt1TrackAllL0` accepts events that were accepted by any L0 channel and that have at least one track that satisfies a number of track quality criteria (see Ref. [9]), that is displaced from every reconstructed PV in the event (impact parameter with respect to each PV > 0.1 mm), and that has a

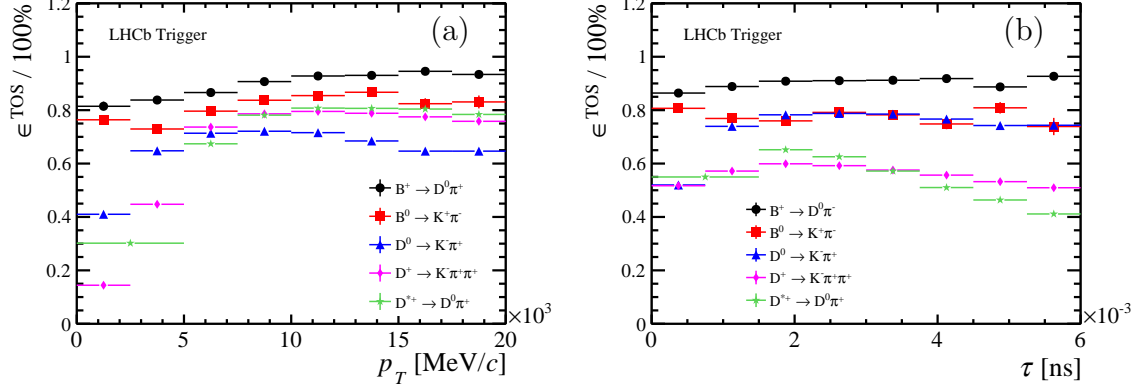


Figure 3: The efficiency Hlt1TrackAllL0 for various reconstructed decay modes as functions of (a) p_T and (b) τ of the signal B or D candidate based on $\sqrt{s} = 8$ TeV data collected in 2012. For the decay mode $D^{*+} \rightarrow \pi^+ D^0 (K^- \pi^+ \pi^+ \pi^-)$, τ is the measured decay time of the D^0 candidate.

relatively large estimated p_T ($p_T > 1.7$ GeV/c). Such tracks are typically produced by the decay products of c and b -hadrons and are excellent signatures of long-lived heavy hadrons.

We evaluate the performance of Hlt1TrackAllL0 relative to the output of L0 with a set of offline candidate decays that are from events accepted by L0 and that are TIS with respect at least one of the HLT1 lines for physics analyses. Figure 3 shows ϵ^{TOS} of Hlt1TrackAllL0 as functions of p_T of the signal candidate and of measured decay time, τ , of the signal D^0 or D^+ candidate for $D^0 \rightarrow K^- \pi^+$, $D^+ \rightarrow K^- \pi^+ \pi^+$, and $D^{*+} \rightarrow \pi^+ D^0 (K^- \pi^+ \pi^+ \pi^-)$ decays. It also shows ϵ^{TOS} of Hlt1TrackAllL0 for two hadronic B decay modes, $B^+ \rightarrow \pi^+ D^0 (K^- \pi^+)$ and $B^0 \rightarrow K^+ \pi^-$. The mean efficiencies for the L0-accepted HLT1-TIS offline candidate decays appear in Table 2.

Table 2: Mean ϵ^{TOS} efficiencies of Hlt1TrackAllL0 relative to L0-accepted events for selected charm hadron decays.

Decay mode	Mean ϵ^{TOS}
$D^0 \rightarrow K^- \pi^+$	0.66853 ± 0.00054
$D^+ \rightarrow K^- \pi^+ \pi^+$	0.58580 ± 0.00014
$D^{*+} \rightarrow \pi^+ D^0 (K^- \pi^+ \pi^+ \pi^-)$	0.60802 ± 0.00038

8 HLT2 performance

Like HLT1, HLT2 is composed of several independent parallel lines, each of which is executed on each event accepted by at least one of the lines of HLT1. The decisions of each of the L0 channels and HLT1 lines are available to HLT2 and can enter the decision making of a line. Also like HLT1, most of the lines of HLT2 begin with a common reconstruction of PVs and charged particle tracks. This reconstruction is more sophisticated, complete, and precise than that used by HLT1 lines, but it also takes more computing power per event. Reference [9] describes the HLT2 reconstruction for data collection in 2011. Several improvements were made to the 2012 HLT2 reconstruction, chief among them a reduction of the minimum p_T for reconstructed charged tracks from 500 MeV/ c to 300 MeV/ c . The HLT deferral system provided the additional computational power necessary for this more complete track reconstruction.

8.1 Exclusive charm hadron lines

HLT2 lines are generally tailored to the needs of groups of analyses. Because the precision and efficiency of HLT2's track reconstruction approach those of LHCb's analysis software, HLT2 lines can use the same methods and selection variables for fully reconstructing signal decays, with the exception of the charged hadron identification. The algorithms for the charged hadron identification require significant computational power and are executed only for a small number of HLT2 lines on a relatively small number of events after extensive filtering. Among the lines for charm hadron physics, only the lines for Λ_c^+ decays used the charged hadron identification.

The mass distributions of Figure 4 demonstrate the purity with which charm hadron decays are reconstructed by their HLT2 lines. We evaluate the performance of these lines relative to the output of HLT1 with sets of offline candidate decays that are from events that are TOS with respect to one of the HLT1 lines for physics and that are TIS with respect at least one of the HLT2 lines for physics. Figure 5 shows ϵ^{TOS} of the HLT2 lines as functions of p_T of the signal candidate and of measured decay time, τ , of the signal D^0 or D^+ candidate. The mean efficiencies for the L0-accepted HLT1-TOS HLT2-TIS offline candidate decays appear in Table 3.

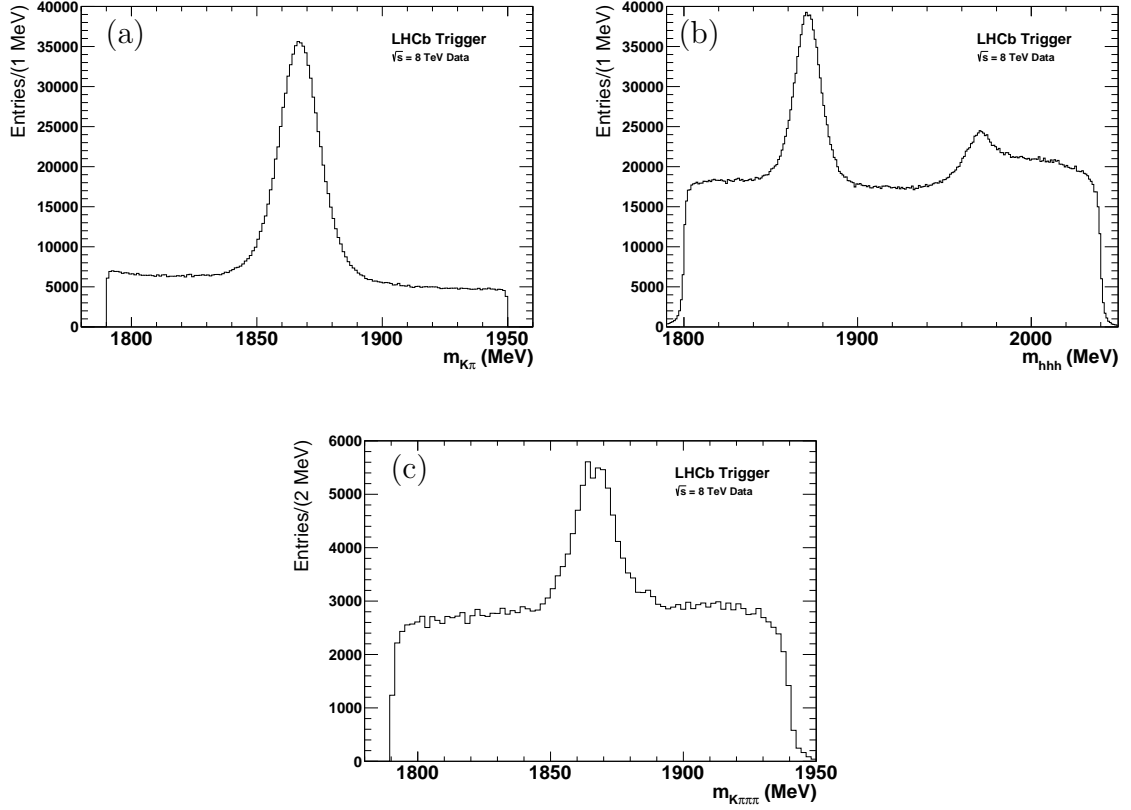


Figure 4: Mass distributions of reconstructed D meson decay candidates in HLT2: (a) $D^0 \rightarrow K^- \pi^+$ candidates reconstructed in the line `Hlt2CharmHadD02HH_D02KPi`, (b) $D_{(s)}^+ \rightarrow h^- h'^+ h''^+$ candidates, where $h, h', h'' \in \{K, \pi\}$, reconstructed in the line `Hlt2CharmHadD2HHH`, and (c) $D^0 \rightarrow K^- \pi^+ \pi^+ \pi^-$ candidates from the $D^{*+} \rightarrow \pi^+ D^0$ candidates reconstructed in the line `Hlt2CharmHadD02HHHHDst_K3pi`.

Table 3: Mean ϵ^{TOS} efficiencies of HLT2 lines relative to HLT1-TOS events for selected charm hadron decays.

Decay mode	HLT2 line	Mean ϵ^{TOS}
$D^0 \rightarrow K^- \pi^+$	<code>Hlt2CharmHadD02HH_D02KPi</code>	0.9069 ± 0.0015
$D^+ \rightarrow K^- \pi^+ \pi^+$	<code>Hlt2CharmHadD2HHH</code>	0.6588 ± 0.0005
$D^{*+} \rightarrow \pi^+ D^0 (K^- \pi^+ \pi^+ \pi^-)$	<code>Hlt2CharmHadD02HHHHDst_K3pi</code>	0.1989 ± 0.0004
	<code>Hlt2CharmHadD02HHXDst_hhX</code>	0.1712 ± 0.0005
	<code>Hlt2CharmHadD02HHHHDst_K3pi</code>	
	or <code>Hlt2CharmHadD02HHXDst_hhX</code>	0.2556 ± 0.0005

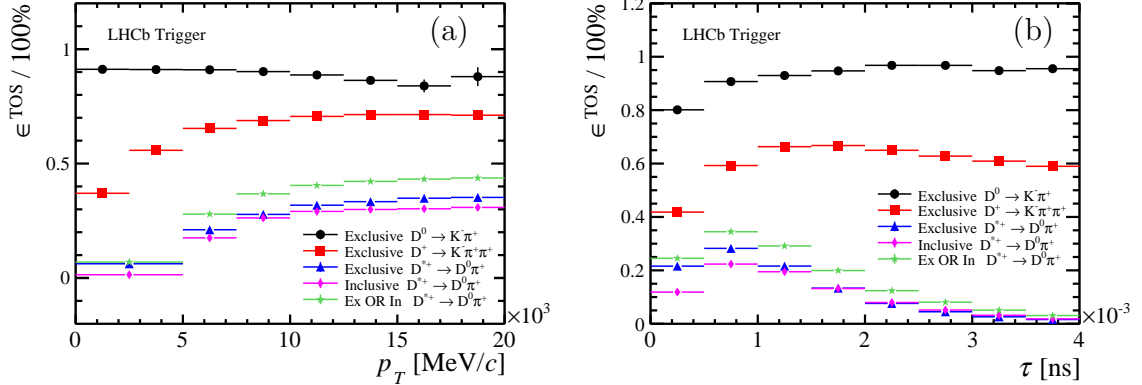


Figure 5: The efficiency of various HLT2 lines for appropriate reconstructed decay modes as functions of (a) p_T and (b) τ of the signal D candidate based on $\sqrt{s} = 8$ TeV data collected in 2012. For the decay mode $D^{*+} \rightarrow \pi^+ D^0 (K^- \pi^+ \pi^+ \pi^-)$, τ is the measured decay time of the D^0 candidate.

8.2 Inclusive D^{*+} line

Although highly successful, HLT2 lines for exclusive reconstruction of decay modes are necessarily limited. Inclusive selections that do not depend on a complete reconstruction of signal decays can allow for efficient selection of a broader range of decay modes, including modes for which a full reconstruction is impossible. The inclusive D^{*+} HLT2 line is a first example of inclusive triggering for charm hadrons.

The inclusive D^{*+} line, `Hlt2CharmHadD02HHXDst_hhX`, selects decays of $D^{*+} \rightarrow \pi^+ D^0$, where D^0 decays into at least two charged final state particles. Partial D^0 decay candidates are reconstructed as two-track vertexes that are significantly displaced from all PVs. These two-track vertexes are combined with π^+ candidates to form D^{*+} candidates, and additional basic kinematic and reconstruction quality criteria are applied to the system. For true D^{*+} decays, the mass difference between the reconstructed D^{*+} and D^0 candidates peaks strongly at the

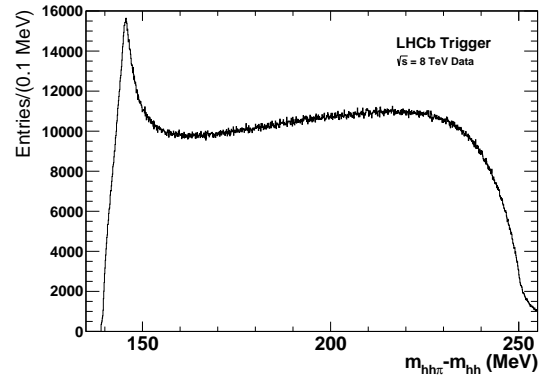


Figure 6: Mass difference distribution of reconstructed candidates for the HLT2 inclusive D^{*+} line `Hlt2CharmHadD02HHXDst_hhX`.

true value, even when the D^0 decays are not fully reconstructed. Thus D^{*+} decays can be successfully identified for a wide array of D^0 decay modes. The method has also been applied to $\Sigma_c^{0(++)} \rightarrow \Lambda_c^+ \pi^{-(+)}$ decay modes with partially reconstructed Λ_c^+ decays in additional HLT2 lines. Figure 6 shows the prominent signal component in the D^{*+} - D^0 candidate mass differences for the D^{*+} candidates selected by the inclusive D^{*+} HLT2 line.

Figure 5 includes a comparison of the performance of the inclusive D^{*+} line with that of the exclusive line for $D^{*+} \rightarrow \pi^+ D^0 (K^- \pi^+ \pi^+ \pi^-)$ decays. The inclusive line has a comparable efficiency and, furthermore, selects a complementary set of decays as can be seen in the efficiencies of Table 3. Approximately 33% of the signal decays selected by the inclusive line were not selected by the exclusive line. Most of these are decays for which one of the final state particles has $p_T < 300 \text{ MeV}/c$, the lower limit for the track reconstruction in the exclusive lines.

9 Future developments

9.1 Post-LS1 LHCb triggering

In 2015 LHCb will resume data collection after LHC's LS1 at the greater pp collision energy of $\sqrt{s} = 13 \text{ TeV}$. The L0 hardware trigger will be tuned to satisfy its 1 MHz output limit under the new conditions, but its operation will remain unchanged. The HLT software trigger will be substantially reorganized in order to improve the quality of the event reconstruction in HLT2.

The internal structures of HLT1 and HLT2 will remain largely unchanged, with the possible addition of lines to expand LHCb's physics program. However, an additional calibration step will be inserted between HLT1 and HLT2. In 2010-2012, the calibration and the fine alignment of detector elements that was used by the HLT2 reconstruction were measured in an earlier data-taking period. Since the calibration and alignment for analysis is always up-to-date, there may be small differences between the measured parameters of identical candidates as reconstructed in HLT2 and as reconstructed for analysis. This can be a source of irreducible systematic uncertainty. By performing the calibration and alignment step before the execution of HLT2, this source of uncertainty is reduced or eliminated.

HLT1 will run immediately on all L0-accepted events. The events accepted by HLT1 will be cached on the storage of the EFF by a system similar to the HLT deferral until an update of the a detector alignment and calibration is complete. Then HLT2 will process the cached HLT1-accepted events and render the final trigger decisions.

9.2 Triggering in an upgraded LHCb detector

Following the conclusion of LHC Run II, the LHCb experiment will be upgraded for a higher rate of data collection [13, 14]. The upgraded experiment will feature a substantially improved trigger. Inefficiency in the L0 trigger is one of the main limitations of the current system for b and c -hadron decays to hadronic final states. This inefficiency is necessitated by 1 MHz maximum readout rate for the detector electronics. The upgraded LHCb detector will be capable of a full detector readout at 40 MHz, largely obviating the need for L0. L0 will be upgraded to a Low Level Trigger that will function as a pass-through during normal operation. All trigger decisions will be made by the more flexible and efficient HLT, which will evolve to process the higher input rate. The rate at which events are accepted by the trigger for permanent storage will increase from the current 5 kHz to an estimated 20 kHz. The combination of a more efficient software trigger and the increased rate of data collection is estimated to increase the annual yield of many charm decay modes by an order of magnitude.

10 Summary

The current performance of the LHCb charm triggering, as documented in this article, is the product of steady iterative improvement made with the goal of expanding the scope and impact of LHCb's physics program. Development of the trigger system continues, with further important enhancements anticipated for LHC Run II and for the subsequent upgrade of the LHCb experiment. The LHCb trigger will continue to deliver world-class charm data sets for many years.

References

- [1] LHCb collaboration, R. Aaij *et al.*, *Measurement of D^0 - \bar{D}^0 mixing parameters and search for CP violation using $D^0 \rightarrow K^+\pi^-$ decays*, [arXiv:1309.6534](#), submitted to Phys. Rev. Lett.
- [2] LHCb collaboration, R. Aaij *et al.*, *Measurement of form factor independent observables in the decay $B^0 \rightarrow K^{*0}\mu^+\mu^-$* , [arXiv:1308.1707](#), to appear in Phys. Rev. Lett.
- [3] LHCb collaboration, R. Aaij *et al.*, *Measurement of $\sigma(pp \rightarrow b\bar{b}X)$ at $\sqrt{s} = 7$ TeV in the forward region*, Phys. Lett. **B694** (2010) 209, [arXiv:1009.2731](#).
- [4] LHCb collaboration, R. Aaij *et al.*, *Prompt charm production in pp collisions at $\sqrt{s} = 7$ TeV*, Nucl. Phys. **B871** (2013) 1, [arXiv:1302.2864](#).

- [5] LHCb collaboration, A. A. Alves Jr. *et al.*, *The LHCb detector at the LHC*, JINST **3** (2008) S08005.
- [6] M. Adinolfi *et al.*, *Performance of the LHCb RICH detector at the LHC*, Eur. Phys. J. **C73** (2013) 2431, [arXiv:1211.6759](#).
- [7] A. A. Alves Jr. *et al.*, *Performance of the LHCb muon system*, JINST **8** (2013) P02022, [arXiv:1211.1346](#).
- [8] LHCb collaboration, R. Antunes-Nobrega *et al.*, *LHCb trigger system : Technical design report*, CERN-LHCC-2003-031 (2003), LHCb TDR 10.
- [9] R. Aaij *et al.*, *The LHCb trigger and its performance in 2011*, JINST **8** (2013) P04022, [arXiv:1211.3055](#).
- [10] LHCb collaboration, B. Adeva *et al.*, *Roadmap for selected key measurements of LHCb*, [arXiv:0912.4179](#).
- [11] LHCb collaboration, R. Aaij, *et al.*, and A. Bharucha *et al.*, *Implications of LHCb measurements and future prospects*, Eur. Phys. J. **C73** (2013) 2373, [arXiv:1208.3355](#).
- [12] L. Evans and P. Bryant, *LHC Machine*, JINST **3** (2008) S08001.
- [13] LHCb collaboration, R. Aaij *et al.*, *Letter of Intent for the LHCb Upgrade*, CERN-LHCC-2011-001, LHCC-I-018 (2011).
- [14] LHCb collaboration, I. Bediaga *et al.*, *Framework TDR for the LHCb Upgrade: Technical Design Report*, CERN-LHCC-2012-007, LHCb-TDR-12 (2012).